

A Common Origin for Aftershocks, Foreshocks, and Multiplets

by Karen R. Felzer,* Rachel E. Abercrombie, and Göran Ekström

Abstract We demonstrate that the statistics of earthquake data in the global Centroid Moment Tensor (CMT) and National Earthquake Information Center (NEIC) catalogs and local California Council of the National Seismic System (CNSS) catalog are consistent with the idea that a single physical triggering mechanism is responsible for the occurrence of aftershocks, foreshocks, and multiplets. Specifically, we test the hypothesis that tectonic earthquakes usually show clustering only as a result of an initial earthquake triggering subsequent ones and that the magnitude of each triggered earthquake is entirely independent of the magnitude of the triggering earthquake. Therefore a certain percentage of the time, as determined by the Gutenberg–Richter magnitude–frequency relationship, an earthquake should by chance be larger than or comparable in size to the earthquake that triggered it. This hypothesis predicts that the number of times foreshocks or multiplets are observed should be a fixed fraction of the number of aftershock observations. We find that this is indeed the case in the global CMT and NEIC catalogs; the average ratios between foreshock, aftershock, and multiplet rates are consistent with what would be predicted by the Gutenberg–Richter relationship with $b = 1$. We give special attention to the Solomon Islands, where it has been claimed that unique fault structures lead to unusually high numbers of multiplets. We use Monte Carlo trials to demonstrate that the Solomon Islands multiplets may be explained simply by a high regional aftershock rate and earthquake density. We also verify our foreshock results from the more complete recordings of small earthquakes available in the California catalog and find that foreshock rates for a wide range of foreshock and mainshock magnitudes can be projected from aftershock rates using the Gutenberg–Richter relationship with $b = 1$ and the relationship that the number of earthquakes triggered varies with triggering earthquake magnitude M as $c10^{\alpha M}$, where c is a productivity constant and α is equal to 1. Finally, we test an alternative model that proposes that foreshocks do not trigger their mainshocks but are instead triggered by the mainshock nucleation phase. In this model, the nucleation phase varies with mainshock magnitude, so we would expect mainshock magnitude to be correlated with the magnitude, number, or spatial extent of the foreshocks. We find no evidence for any of these correlations.

Introduction

The term “aftershocks” is generally used to refer to a cluster of smaller earthquakes following a larger one, which is referred to as the “mainshock.” Clusters of earthquakes of comparable size are referred to as “multiplets” (or “doublets,” for pairs of events), and clustered smaller earthquakes preceding a larger one are called “foreshocks.” There is general agreement that aftershocks are triggered by stress changes (of some sort) induced by the mainshock’s rupture. Some researchers argue, however, that the physics behind

multiplets and foreshocks is different than that for aftershocks, with multiplets being especially prevalent only where seismic zones contain large, simple asperities, as has been suggested by Lay and Kanamori (1980), and foreshocks occurring because they are triggered by the nucleation phase of the upcoming mainshock (Ohnaka 1993; Dodge *et al.*, 1995; Hurokawa 1998).

Other researchers argue that the magnitude of a triggered earthquake is independent of the magnitude of the earthquake that triggered it, and thus what we see as aftershocks, multiplets, and foreshocks actually represent a single triggering process. In this model, when an earthquake occurs, it may trigger slip on small fault patches surrounding

*Present address: Department of Earth and Space Sciences, 3806 Geology Building, University of California, Los Angeles, Box 951567, Los Angeles, California 90095-1567.

the hypocenters of future earthquakes. The number of hypocenters triggered, n , is given by

$$n = c10^{\alpha M}, \quad (1)$$

where M is the magnitude of the triggering earthquake, c is a productivity constant, and α is a parameter that controls the relative number of aftershocks triggered as a function of mainshock magnitude. In this model, each triggered earthquake then grows to a magnitude randomly chosen from the Gutenberg–Richter magnitude–frequency relationship, which gives that $\log(N) = a - bm$, where N is the number of earthquakes larger than or equal to magnitude m , b is a constant typically close to unity, and a is a constant that depends on the local activity rate (Ishimoto and Iida, 1939; Gutenberg and Richter, 1944). This single-process triggering model has been used to build statistical models of seismicity (Vere-Jones, 1966; Kagan and Knopoff, 1981; Ogata, 1988; Helmstetter and Sornette, 2002), to analyze earthquake clustering (Console and Murru, 2001), to estimate the prevalence of secondary aftershocks (Felzer *et al.*, 2002), to study foreshocks (Shaw, 1993; Jones *et al.*, unpublished manuscript), and to find the average time-dependent risk in California of a large earthquake being triggered by recent seismic activity (Reasenber and Jones, 1989).

The purpose of this article is to use earthquake statistics, derived from the global International Seismological Centre (ISC) and National Earthquake Information Center (NEIC) catalogs and regional California Council of the National Seismic System (CNSS) catalog, to investigate whether aftershocks, multiplets, and foreshocks represent a single physical processes or multiple ones. In order to perform this investigation, it is necessary to set a value for α in equation (1) and a value for b in the Gutenberg–Richter equation. We follow Reasenber and Jones (1989), Michael and Jones (1998), Console and Murru (2001), and Felzer *et al.* (2002) and set $\alpha = b$ because this allows for the reproduction of Båth’s law, an empirical relationship that states that the average magnitude difference between a mainshock and its largest aftershock is independent of mainshock magnitude (Utsu, 1961; Båth, 1965; Tapanos, 1990; Felzer *et al.*, 2002). In addition, setting $\alpha = b$, or more precisely setting $\alpha = b = 1.0$, which is the typically observed b -value, is consistent with California aftershock counts, as we will demonstrate later, and means (assuming constant stress drop) that aftershock production varies directly with mainshock faulting area, which agrees with empirical observations (Yamanaka and Shimazaki, 1990; Jones and Hauksson, unpublished manuscript). Other values for α given in the literature include 0.5 (Console *et al.*, 2003) and 0.8 (Helmstetter, 2003). In the rest of this article we will refer to the single physical model for earthquake triggering, along with the stipulations that $\alpha = b = 1.0$ and that α and b remain invariant with time, as the “single-mode triggering model.”

In this article we use the single-mode triggering model to make four predictions. We then test if these predictions

are supported by the data, testing the first two predictions with the global data set and the second two predictions with the California earthquake catalog. We also perform additional tests to see whether it is possible to disprove the idea that a single triggering mechanism is all that is necessary to explain the observed earthquake statistics.

Predictions of the Single-Mode Triggering Model

We make four predictions using the single-mode triggering model. The first is that since the model holds that aftershocks and doublets result from the same triggering process, regional aftershock and doublet rates should vary linearly with each other. For example, where aftershock rates are low doublet rates should also be low, and so on.

The second prediction is that, for the same reason, aftershock and foreshock rates should vary linearly with each other. Thus, significant regional variations in the rate of foreshock occurrence as observed, for example, by Reasenber (1999), may be simply explained by regional variations in earthquake-triggering efficiency and should correlate directly with aftershock rate variability.

Our third prediction is that aftershock production should vary with mainshock magnitude, M_1 , as $c10^{\alpha M_1}$ where c is a constant and $\alpha = 1.0$. Therefore, if we count aftershocks above some set cutoff magnitude M_2 , the number of aftershocks larger than or equal to M_2 , $N(m \geq M_2)$, should be given by

$$N(m \geq M_2) = c10^{M_1}, \quad (2)$$

where M_2 may be either smaller or larger than M_1 .

Our fourth prediction is that the number of aftershocks having a magnitude $M_2 \pm \Delta M$, where M_2 is now a variable rather than a fixed value, should vary as

$$N(M_2 \pm \Delta M) = C10^{b(M_1 - M_2)}, \quad (3)$$

where C is a constant and $b = 1.0$. This prediction is arrived at by multiplying together prediction 3, that the number of triggered earthquakes should vary as 10^{M_1} , with the specification that the magnitude of each triggered earthquake is chosen randomly from the Gutenberg–Richter relationship, which gives that the probability of having an earthquake of magnitude M_2 is $10^a \times 10^{-M_2}$. A similar prediction was made and investigated by Michael and Jones (1998).

Testing the Predictions of the Single-Mode Triggering Model

Data Processing

To test the first two predictions of the single-mode triggering model, we need to compare different regions with aftershock, doublet, and foreshock rates that vary significantly. This requires use of a global catalog. To keep mag-

nitude measurements as consistent as possible, we use moment magnitudes from the Harvard Centroid Moment Tensor (CMT) catalog from 1976 through 2001. The Harvard CMT catalog is generally complete down to M_w 5.6, but earthquakes larger than M_w 5.6 may be missed if they occur too soon after previous large earthquakes. Thus we compare the NEIC and CMT catalogs and add in NEIC data for earthquakes found to be missing in the CMT catalog. The magnitudes used from the NEIC catalog are generally M_S . If M_S is not available, m_b is used instead. Even with the combined catalog some smaller aftershocks above the normal catalog completeness level are still missed, so we only count triggered earthquakes that are no smaller than 1 magnitude unit less than their trigger.

In processing the data each earthquake is treated as a potential mainshock unless it participates in the first 30 days of the aftershock sequence of a larger earthquake. Early aftershocks of larger earthquakes are not considered as potential mainshocks because they often occur among such active seismicity that it is difficult to determine their specific relationships with other earthquakes.

For each earthquake that is considered a potential mainshock, we search for triggered earthquakes for the following 2 days in a box that is centered on the earthquake's epicenter. The distance from the earthquake's epicenter to the side of the box is set equal to 2.5 times the earthquake's estimated fault length (using the equations of Kanamori and Anderson [1975] assuming a circular rupture and a constant stress drop of 30 bars). The metric of 2.5 times the fault length is chosen because aftershocks are generally held to occur within 2 fault lengths; the extra half a fault length is added on because of significant location error in the global catalog. The time period of 2 days is chosen because many of the doublets cited in the literature occur within 2 days of each other (Lay and Kanamori, 1980; Schwartz and Coppersmith, 1984; Xu and Schwartz, 1993). In addition, using a short time window reduces the chances of including too many background earthquakes. If a particular earthquake is claimed as the aftershock of multiple mainshocks, it is assigned to the largest mainshock.

The earthquakes in each cluster are then classified according to their relative magnitudes. Many doublets cited in the literature are within ± 0.4 magnitude units of each other (Lay and Kanamori, 1980; Schwartz and Coppersmith, 1984; Xu and Schwartz, 1993), so all clustered earthquakes that are within 0.4 magnitude units of each other are classified as doublets. Since the smallest earthquake we count is M 5.6, this means that to ensure catalog uniformity the smallest earthquake we can consider as a potential doublet initiator is M 6.0. Each earthquake pair that meets the criteria is counted as one doublet, so if we have a multiplet sequence with three earthquakes this is counted as two doublets, and so on. All earthquakes that are 0.4–1.0 magnitude units smaller than the cluster-initiating mainshock are classified as aftershocks. This differs with the general definition of an aftershock as anything smaller than the mainshock; but since

we wish to compare aftershock and doublet rates, the two data sets cannot be allowed to overlap. Since the smallest earthquake we count is M 5.6, again to ensure catalog uniformity earthquakes classified as aftershocks must be preceded by an initial mainshock at least as large as M 6.6 (so that we do not need to search for any aftershocks smaller than M 5.6). Finally, we classify all cluster-initiating earthquakes that are smaller than a following earthquake as foreshocks. There is some overlap, therefore, between the foreshock and doublet data sets, but this will not bias our results since we do not plan to directly compare the foreshock and doublet rates. Note that earthquakes counted as foreshocks may be as small as M 5.6.

For the third and fourth predictions it is not necessary to compare different regional aftershock rates, so we can use a single regional data set with a large amount of quality data. We chose the CNSS California catalog, using data from 1975 through 2001, a period during which much of the catalog was complete down to M_L 2.1 or 2.2. We use earthquakes down to M_L 2.2 for our calculations. We exclude data from the Mammoth Lakes volcanic region out of concern that movements of magma and other volcanic processes may cause seismicity in this region to show different properties than in other regions of California. Because California location quality is much better than for the global catalog (on the order of 2 km rather than 20 km), we also search for aftershocks in a box centered on the mainshock's epicenter with a half-length that is only 2 times, rather than 2.5 times, the estimated mainshock fault length. Because of location concerns, however, the half-length of the box is fixed at 2 km for mainshocks with fault lengths smaller than 1 km (e.g., earthquakes smaller than about M_L 3.9).

Testing Prediction 1: Are Multiplets Just Large Aftershocks?

We test the first prediction of the single-mode triggering model by plotting the number of aftershocks per mainshock versus the number of doublets per mainshock in different global seismic regions (Fig. 1). We observe a statistically significant (95% confidence) correlation between the global doublet and aftershock rates ($r = 0.6$). Because the single-mode triggering model predicts that the magnitude of each triggered earthquake should be chosen randomly from the Gutenberg–Richter distribution, we predict that the relative probability that a triggered earthquake will be within ± 0.4 magnitude units of the mainshock versus the probability that it will be 0.4–1.0 magnitude units smaller than the mainshock should be given by

$$(10^{0.4} - 10^{-0.4}) / (10^1 - 10^{0.4}) = 0.28. \quad (4)$$

Therefore we predict that

$$\text{doublet rate} = 0.28 \times \text{aftershock rate}. \quad (5)$$

This line, plotted in Figure 1, constitutes a relatively good

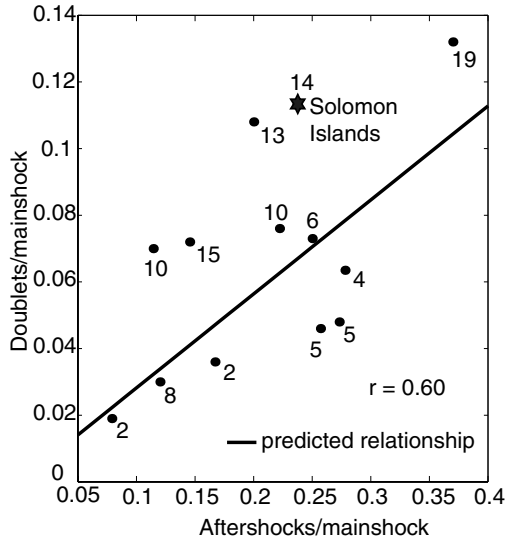


Figure 1. The number of doublets per mainshock is plotted against the number of aftershocks per mainshock for the Kuriles, the Solomon Islands, New Hebrides, the Phillipines, the Aleutians, New Zealand, Sumatra, the west coast of North America, Japan, South America, midoceanic ridges, Tibet, and Italy. Data are taken from the CMT and NEIC catalogs from 1976 to 2001. Aftershocks and doublets are defined as $M \geq 5.6$ earthquakes occurring within 2 days and 2.5 fault lengths of mainshocks, where aftershocks are 1.0–0.4 magnitude units smaller than their mainshocks (which thus must be $M \geq 6.6$) and doublets are within ± 0.4 magnitude units of their mainshock (which must be $M \geq 6.0$). The numbers by each data point indicate the raw number of doublets in each region. The doublet and aftershock rates are positively correlated at the 95% confidence level with a correlation coefficient of $r = 0.6$. The relationship between the doublet and aftershock rates predicted by the single-mode triggering model is given by the solid line.

fit, with seven data points plotting above the line and six points plotting below. Performing a χ^2 test indicates that this line cannot be rejected as the function that describes the data set at the 95% confidence level. We can also test equation (5) by averaging together the entire data set, which consists of 700 potential mainshocks. We find an overall average aftershock rate of 0.202 aftershocks/mainshock. Thus equation (5) (combined with binomial probability) predicts that the average doublet rate should be 0.057 ± 0.015 doublets/mainshock (98% confidence interval). We measure an actual average doublet rate of 0.0694 doublets/mainshock, which is within these confidence limits.

Yet although the data as a whole appear to agree well with the single-mode triggering model, the individual data points clearly show a large amount of scatter. This is to be expected because of the small size of the regional data sets (see Fig. 1) and problems associated with regionally variable location and magnitude errors. But it may also be because in a few cases some unusual tectonic properties introduce

special physics that cause large earthquakes to be more likely to be followed by other large earthquakes. Such a physical mechanism has been proposed in particular for the Solomon Islands, where Lay and Kanamori (1980) hypothesized that the high rate of multiplets is caused by the regional occurrence of large, simple asperities lined up along the subduction zone.

The Solomon Islands do have one of the largest doublet rates in the world (Fig. 1). If we only consider earthquakes $M \geq 7$, in fact, the Solomon Islands have had the largest doublet rate of any region we have inspected over the last 25 years. Yet the Solomon Islands also have a high aftershock rate. In addition, we calculate that the Solomon Islands have the third highest earthquake density in the world and that the only two regions with higher densities (the Kuriles and the New Hebrides trench) also have high doublet rates. We measure earthquake density by covering a seismic region with a rectangle large enough to enclose all of the seismicity, breaking the rectangle into 50 by 50 km squares, and then taking the ratio of the total number of earthquakes in the rectangle to the total number of 50 by 50 km squares that contain earthquakes.

The principal question is whether the number of doublets observed in the Solomon Islands is within the expected range of variability predicted by the single-mode triggering model given the high regional aftershock rate, high earthquake density, and the earthquake magnitude distribution normally recorded in the region, or whether the doublet rate is high enough to disprove the single-mode triggering model. We approach this question by running 10,000 Monte Carlo trials. The input for each trial is the number of $M \geq 6$ earthquakes occurring in the Solomon Islands between 1976 and 2002, the aftershock rate of $M \geq 6$ earthquakes measured in the Solomon Islands, and the magnitude distribution of $M \geq 6$ earthquakes recorded there. We then run simulations using the single-mode triggering model equations and count how many doublets are randomly produced by the model in each trial.

Among 57 $M \geq 6.0$ earthquakes actually occurring in the Solomon Islands between 1976 and 2002, 6 were observed to have doublets. In our random simulations, six or more doublets are produced 38% of the time. Among 16 $M \geq 7.0$ earthquakes occurring since 1976 in the Solomon Islands, 4 had doublets; in our simulations 4 or more $M \geq 7$ doublets are produced by chance 18% of the time. We use the same method to test the high doublet rates in New Hebrides and the Kuriles. In New Hebrides, 10 of 69 $M \geq 6$ mainshocks had doublets during our study period; our simulations indicate a 13% probability of this occurring by chance under the single-mode triggering model. In the Kuriles, 7 of 46 $M \geq 6$ mainshocks had doublets; we calculate that this has a 5% probability of occurring by chance. Therefore it appears that no global tectonic region has a doublet rate high enough to clearly disprove the single-mode triggering model.

Testing Predictions 2–4: Are Foreshocks Just Small Mainshocks?

Testing Prediction 2 with the Global Data Set. We test the second prediction of the single-mode triggering model by plotting the number of foreshocks per mainshock versus the number of aftershocks per mainshock in different regions, and we find that aftershock and foreshock rates do vary linearly with each other (Fig. 2). Using the same method as in the Predictions section, we calculate that theoretically according to the single-mode triggering model,

$$\text{foreshock rate} = 0.134 \times \text{aftershock rate}. \quad (6)$$

The χ^2 test indicates that this line cannot be rejected as the function that defines the data set at the 95% confidence level. Since we have calculated that the globally averaged aftershock rate is 0.202 aftershocks/mainshock, equation (6) and binomial probability also predict that the globally averaged foreshock rate should be 0.0271 ± 0.0104 foreshocks/mainshock (98% confidence intervals). We measure an actual average of 0.0238 foreshocks/mainshock, which is well within these confidence limits. However, the scatter for the individual data points is larger than for the aftershock versus doublet plot, probably because there are fewer foreshocks than there are doublets, and the correlation is significant only at the 90% confidence level ($r = 0.46$). Luckily we can also test the foreshock component of the single-mode triggering model with a more comprehensive data set from a single region via the third and fourth predictions of the single-mode triggering model. We do so in the next section.

Testing Predictions 3 and 4 with the California Data Set.

For the third and fourth predictions, we use the more comprehensive California earthquake catalog. For the test of the third prediction, we count triggered earthquakes that are larger than $M_L 4.5$ as a function of the magnitude of their potential trigger (Fig. 3). On the left-hand side of the dotted line in Figure 3A are potential triggering earthquakes smaller than $M_L 4.5$ (i.e., foreshocks); on the right-hand side of the line are potential triggering earthquakes larger than $M_L 4.5$. We see that on both sides of this line the number of $M_L \geq 4.5$ triggered earthquakes increases with the magnitude of the potential triggering earthquake and that the rate of increase agrees well with that predicted by the single-mode triggering model (given by the solid line in the figure). We choose $M_L 4.5$ as the lower bound for the triggered earthquakes because it lies in the middle of the magnitude range being tested, leaving plenty of room for both foreshocks and aftershocks. If we lower the magnitude threshold, we increase the number of earthquakes that may be triggered and agreement with the single-mode triggering model improves with the larger data set (Fig. 3B).

Since Figure 3 gives information about how the triggering ability of an earthquake changes as a function of its magnitude, we can also use this data to test our assumption

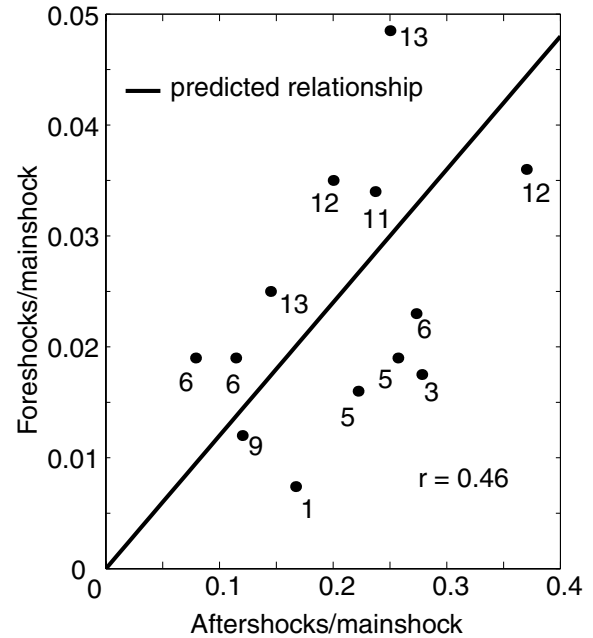


Figure 2. The number of foreshocks per mainshock plotted against the number of aftershocks per mainshock for the Kuriles, the Solomon Islands, New Hebrides, the Phillipines, the Aleutians, New Zealand, Sumatra, the west coast of North America, Japan, South America, midoceanic ridges, Tibet, and Italy. Data are taken from the CMT and NEIC catalogs from 1976 to 2001. Aftershocks are defined as earthquakes that are 1.0–0.4 magnitude units smaller than and occur within 2 days and 2.5 fault lengths of $M \geq 6.6$ mainshocks. Foreshocks are any $M \geq 5.6$ earthquakes that are smaller than and occur up to 2 days before and within 2.5 fault lengths of other $M \geq 5.6$ earthquakes. The numbers by each data point indicate the raw number of earthquakes with foreshocks in each region. The foreshock and aftershock rates are positively correlated at the 90% confidence level with a correlation coefficient of $r = 0.46$. The relationship between the foreshock and aftershock rates predicted by the single-mode triggering model is given by the solid line.

that it is reasonable to set the α parameter in the single-mode triggering model, which controls the relative ability of earthquakes of different magnitudes to produce aftershocks, to 1.0 (equation 1). Specifically, we use the number of $M \geq 3.5$ aftershocks produced by each 0.2 magnitude ranges, as given in Figure 3B. We do the test by varying α in increments of 0.02. For each value of α we calculate an optimal productivity constant c (equation 1) by taking the mean of c values preferred by each data point. Then we calculate the summed least-squares error between the theoretical relationship and the data for each value of α (Fig. 4). We find that the least-squares error is lowest for $\alpha = 0.98$, but it is nearly as low for $\alpha = 1.0$ and $\alpha = 1.02$. Values further away from 1.0 in either direction produce progressively worse fits. Thus we feel justified in setting α to 1.0.

Finally, we test the fourth prediction of the single-mode

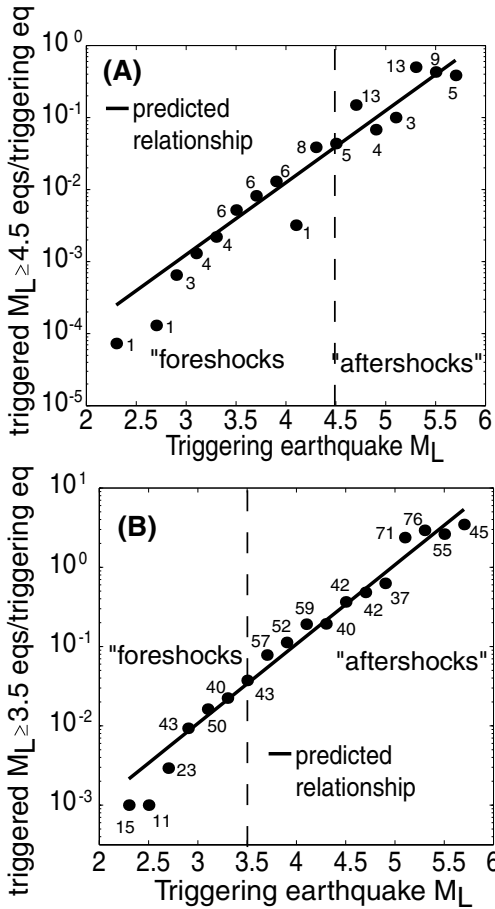


Figure 3. (A) Magnitude of the potential triggering earthquakes plotted against the number of $M_L \geq 4.5$ triggered earthquakes per triggering earthquake. Data are taken from California (excluding the Mammoth Lakes area) and western Nevada from 1975 to 2001. Data from this entire area are used for $M_L \geq 2.6$ triggering earthquakes; for $2.2 \leq M_L < 2.6$ triggering earthquakes areas of far northern and northeastern California and western Nevada, for which the data are not complete below $M_L 2.6$, are not used. Triggering earthquakes are all of the recorded earthquakes in the chosen region minus those earthquakes occurring within the first 30 days of the aftershock sequence of a larger earthquake. The number of triggering earthquakes ranges from 13,761 for $2.2 \leq M_L < 2.4$ to 13 for $5.6 \leq M_L < 5.8$ earthquakes. The raw number of triggered earthquakes (earthquakes occurring within 2 fault lengths and 2 days of a trigger) is written next to each point on the graph. The dotted vertical line separates traditional foreshocks (to the left) from traditional aftershocks (to the right). Note this line signifies no break in the relationship. $M_L 4.5$ is chosen for counting triggered earthquakes because it is near the middle of the magnitude range, but there are not many $M_L \geq 4.5$ earthquakes. The scatter of the data points was reduced in (B) by lowering the triggered earthquake threshold to $M_L 3.5$.

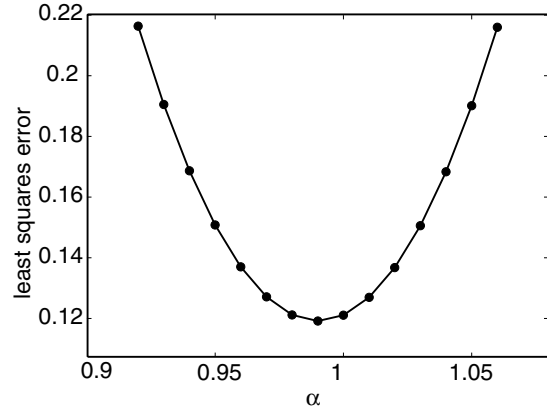


Figure 4. The single-mode triggering model states that aftershock production should vary with mainshock magnitude as $c10^{\alpha M}$, where c is a productivity constant and $\alpha = 1$. We use the number of earthquakes triggered by earthquakes in different magnitude ranges, as given in Figure 3B, to test the $\alpha = 1$ assumption by finding the least-squares misfit between the data and model equation for different values of α . The misfit is lowest at $\alpha = 0.98$, but not dissimilar from the error produced at $\alpha = 1.0$ and $\alpha = 1.02$. Values of α far from 1.0 are unlikely.

triggering model (Fig. 5). The solid line in the figure gives the relationship predicted by the single-mode triggering model for the number of aftershocks as a function of the relative difference between mainshock and aftershock magnitude. Again the model prediction and data show good agreement. There is also no kink or offset in the data as it crosses from the left-hand side of the graph, where the mainshocks are larger than the triggered earthquakes, to the right-hand side, where the mainshocks are smaller than the triggered earthquakes. This provides additional support for the concept that foreshocks, mainshocks, and aftershocks are produced by the same physical mechanism.

We also note that the fourth prediction of the single-mode triggering model is calculated with a b -value of 1.0, or in other words by assuming that the Gutenberg–Richter relationship b -value for the aftershock population is the same as for the earthquake population as a whole. The good fit of the model to the data therefore also lends support to the assumption that $b = 1$. Indeed, we note that because the sum of two power laws with different exponents is not a power law itself, the fact that the entire earthquake population follows the Gutenberg–Richter distribution requires all subpopulations (such as aftershock sequences), which also follow the Gutenberg–Richter distribution, to have identical b -values (Woo, 1996).

Alternate Foreshock Models: Can Single-Mode Triggering be Disproven?

We have shown that all of the predictions made by the single-mode triggering model are consistent with the data. However, agreement with predictions alone is often not

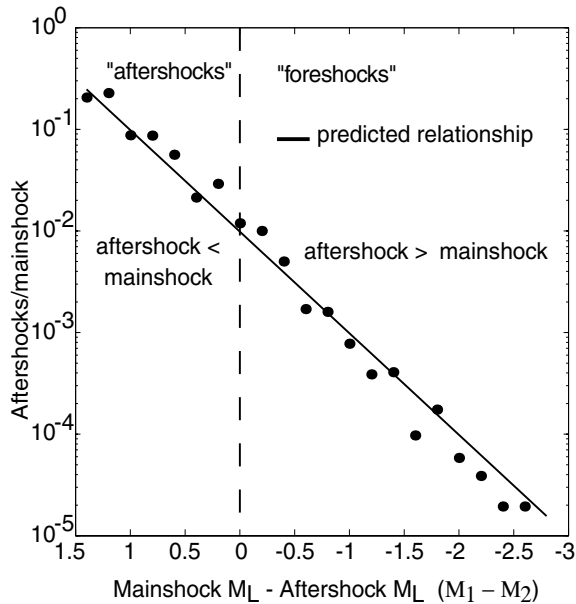


Figure 5. The average number of aftershocks/mainshock if plotted against different values of $M_1 - M_2$ incremented in steps of 0.2 magnitude units. The data set is composed of 101,680 $M \geq 2.2$ California earthquakes (1975–2001). The solid line gives the relationship predicted by the single-mode triggering model. Note that there is no kink or offset in the data as it traverses from the right-hand side of the graph, where the mainshocks are larger than the aftershocks, to the left-hand side of the graph, where the mainshocks (e.g., foreshocks) are smaller than the aftershocks.

enough to prove a model, and there are strong alternate models for why foreshocks occur. Namely, the argument is frequently made that foreshocks are actually triggered by the nucleation phase of the larger earthquake that follows (Ohnaka, 1993; Dodge *et al.*, 1995, 1996; Hurukawa, 1998). For the rest of this section we will refer to this larger following earthquake as the mainshock, as is customary in the literature. The argument by Dodge *et al.* (1995, 1996) that foreshocks could not have triggered the mainshock is based on demonstrations in several test cases that foreshocks did not appear to have increased static stress at the mainshock hypocenter. Nor was there clear static stress transfer evidence for the foreshocks triggering each other. However, up to 30%–40% of even traditional aftershocks often cannot be readily linked to their mainshocks via positive static stress change transfer (Hardebeck *et al.*, 1998). This highlights many problems with current static stress transfer calculations with respect to earthquake triggering, including uncertainties concerning parameters, mainshock rupture, and the effects of small earthquakes, and the essential problem that it is still unknown whether static or dynamic stress changes are actually the primary agents in earthquake triggering (Kilb *et al.*, 2000). Finally, Dodge *et al.* (1995, 1996) assumed circular rupture patches for all of the foreshocks. In the case of

the Joshua Tree foreshock sequence, Mori (1996) demonstrated that relaxing this assumption and inverting for the slip pattern of the largest foreshock reverses the original conclusions.

Another argument commonly made in support of a special origin for foreshocks, that foreshock properties appear to be different from those of other earthquakes, has been refuted by Helmstetter and Sornette (2003). They demonstrated that the commonly observed anomalous behaviors of variations in the b -value in foreshock sequences and accelerations of the seismicity rate before the mainshock are actually artifacts of data-stacking methods used and of not taking into account the effect of aftershocks triggering each other. If foreshocks and foreshock clusters are indeed indistinguishable from other earthquakes, the idea that foreshocks are triggered by the mainshock nucleation phase must be evaluated by testing the central prediction of this model, that foreshock characteristics should scale with mainshock size. This scaling should occur because if the mainshock nucleation phase indeed triggers foreshocks, then the mainshock nucleation phase itself must scale with mainshock size. If it did not, foreshock magnitude could not be controlled by mainshock magnitude; that is, the foreshocks could just as easily end up being larger than the mainshock as smaller than it. Nucleation-phase scaling has also been proposed based on other evidence (Ellsworth and Beroza, 1995). There are three ways in which a scaling nucleation phase might cause foreshock characteristics to scale with mainshock magnitude. Larger mainshocks might be preceded by (1) larger foreshocks, (2) more numerous foreshocks, (3) foreshocks that cover a larger area, or (4) some combination thereof. In the remainder of this section, we will investigate whether any of these types of foreshock scaling can be observed.

Foreshock Magnitude. Previous studies have shown that there is no correlation between mainshock magnitude and the magnitude of the largest foreshock (Agnew and Jones, 1991; Abercrombie and Mori, 1996; Reasenber, 1999; Helmstetter and Sornette, 2003). However, the studies of Agnew and Jones (1991) and Abercrombie and Mori (1996) contained several potential sources of bias. The first is that typically a fixed and relatively small area around the mainshock epicenter was used to search for foreshocks. If foreshocks are actually triggered by the mainshock nucleation phase, using a fixed search area may cause some foreshocks of larger earthquakes to be preferentially missed, especially since the main slip in a large earthquake may occur at some distance from the hypocenter. To decrease this potential bias, we search for foreshocks in a box centered on the mainshock epicenter that has a half-length equal to the mainshock's estimated fault length.

The second potential source of bias is that a hard magnitude cutoff between foreshocks and mainshocks was typically used. In Abercrombie and Mori (1996), for example, earthquakes larger than M_L 5 were only counted as main-

shocks and earthquakes smaller than M_L 5 only as foreshocks. Thus if a mainshock had a foreshock larger than M_L 5, that data point was not included, potentially biasing results. Yet allowing foreshocks to be larger than some of the mainshocks in the data set would, of course, have caused some automatic correlation between mainshock and foreshock magnitude simply because by definition a larger mainshock is capable of having a larger foreshock (for additional treatment of this problem, see Helmstetter and Sornette [2003]).

We address this problem by not testing for direct correlation between foreshock and mainshock magnitude but instead testing whether the probability of having a large foreshock increases with mainshock magnitude. This is done by testing for correlation between the magnitudes of $M_L \geq 4.5$ mainshocks and the fraction of these mainshocks having at least one $M \geq 2.2$ foreshock but no $M > 4.5$ foreshocks. A negative correlation between these variables is expected if the probability of having an $M > 4.5$ foreshock increases with mainshock magnitude, since in this case as mainshock magnitude increases an increasing fraction of mainshocks should have at least one $M > 4.5$ foreshock. It can be seen that in fact there is no statistically significant trend (Fig. 6). This indicates that, at least according to the data that we currently have available, there is no correlation between mainshock and foreshock magnitudes.

Number of Foreshocks. The next question is whether mainshock magnitude influences the number of foreshocks. We plot mainshock magnitude against the number of $2.2 \leq M_L \leq 4.5$ foreshocks occurring before each mainshock (Fig. 7). We only use foreshocks from sequences in which the largest foreshock is $M_L \leq 4.5$, again to prevent the automatic correlation that would occur if larger mainshocks were allowed to have larger foreshocks, and these larger foreshocks in turn triggered larger foreshock sequences. The restriction that the largest foreshock magnitude be smaller than M_L 4.5 does not bias our results because we have already verified an absence of correlation between mainshock and foreshock magnitude. We find no correlation between the number of foreshocks and mainshock magnitude.

Foreshock Area. Finally, we need to test whether mainshock magnitude influences the area spanned by the foreshock cluster. The idea that the area covered by foreshocks scales with mainshock magnitude was suggested by Dodge *et al.* (1996), who found some correlation for six California sequences. This data set was too small, however, to produce significant results. We use the larger data set of foreshocks of all $M \geq 4.6$ California mainshocks (outside of the Long Valley volcanic region), although we do not relocate any of the foreshocks, as was done by Dodge *et al.* (1996).

In order to avoid bias for this particular test, it is necessary to drop the convention of counting foreshocks in an area that scales with mainshock magnitude. Instead, we need to search for foreshocks in an area that is large enough such

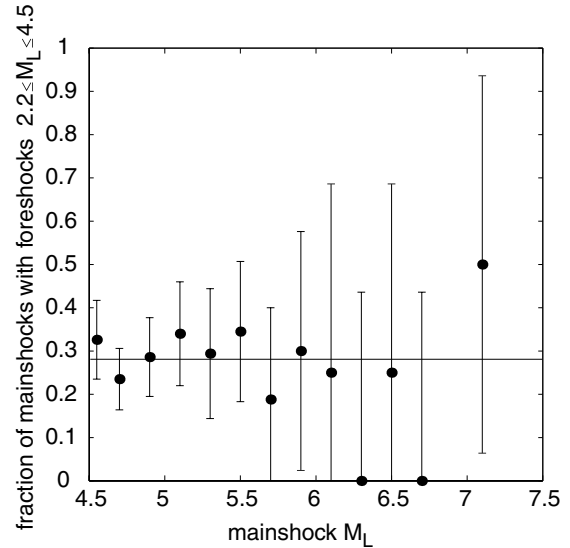


Figure 6. Mainshock magnitude plotted versus the fraction of mainshocks with at least one $M \geq 2.2$ foreshock but no $M > 4.5$ foreshocks. Each data point is plotted with 98% confidence error bars, calculated from binomial probability, based on the number of mainshocks in that magnitude range. If the the probability of having a large foreshock increases with mainshock magnitude, we would expect to see a decreasing trend on this graph (the larger mainshocks would have a larger chance of having at least one $M > 4.5$ foreshock). Instead, there is no statistical correlation between the two variables ($r = -0.18$ for 13 data points, a value that has a 55% probability of occurring by chance.) This indicates that mainshock magnitude does not influence foreshock magnitude.

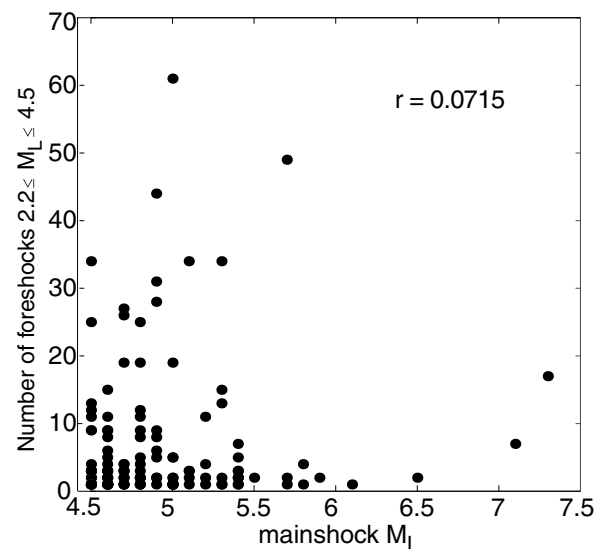


Figure 7. Mainshock magnitude is plotted versus the number of $2.2 \leq M \leq 4.5$ foreshocks in each sequence. No significant correlation between the two variables is seen ($r = 0.07$ for 137 data points, a value that has a 42% probability of occurring by chance), indicating that mainshock magnitude does not influence the number of foreshocks.

that we expect to find all or the vast majority of the foreshocks of the largest mainshocks, but small enough such that we do not end up defining too many random earthquakes as foreshocks. Eliminating spurious foreshocks is particularly important because for this test a few random scattered earthquakes could cause serious overestimation of foreshock-sequence spatial extent. A plot of the distances between individual foreshocks and the mainshock epicenter indicates that the incidence of foreshocks drops off rapidly with distance from the mainshock epicenter from about 0 to 10 km, after which the foreshock counts level off and become erratic (Fig. 8). This suggests that background activity predominates beyond 10 km. Therefore for the purposes of this test, we define anything as a foreshock that occurs within 2 days and 10 km of the mainshock epicenter.

To measure the area covered by each foreshock cluster, we measure the radius of the smallest circle necessary to span each cluster, in map view (Fig. 9). In cases where there is only one recorded foreshock, a radius of 0 km is assigned. We find a total of 88 foreshock sequences, 59 of which have more than one recorded foreshock. We find no significant correlation between foreshock sequence area and mainshock magnitude ($r = -0.06$). The variables remain uncorrelated when the single-foreshock sequences are removed from the

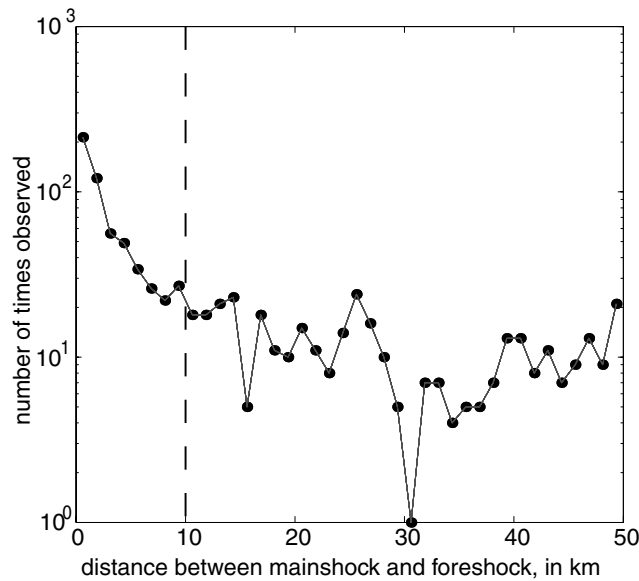


Figure 8. Distance in kilometers between individual foreshock and mainshock epicenters, plotted versus the frequency with which this distance is observed. All foreshocks tabulated occur within 2 days of their mainshock. The incidence of foreshocks falls off as a roughly power-law decay with distance from the mainshock epicenter until about 10 km (vertical line), when it becomes erratic. This suggests that many real foreshocks occur within a 10-km radius of the mainshock epicenter, with most earthquakes occurring at further distances simply being random associates. The data points are calculated from over 900 $M \geq 2.2$ earthquakes.

data set. Conversely, correlation between the largest foreshock in each sequence and the foreshock sequence area, which is expected under the single-mode triggering model since the largest foreshock is expected to trigger many of the others, is found to be significant at over the 99% confidence level ($r = 0.47$). This correlation also remains significant when the single-foreshock sequences are removed. Therefore we conclude that the final prediction of the foreshock challenge, that foreshock area should scale with mainshock magnitude, is not supported by the data.

Conclusions

We find that regional aftershock, doublet, and foreshock rates correlate with each other worldwide. We also find that the number of aftershocks produced by a mainshock of mag-

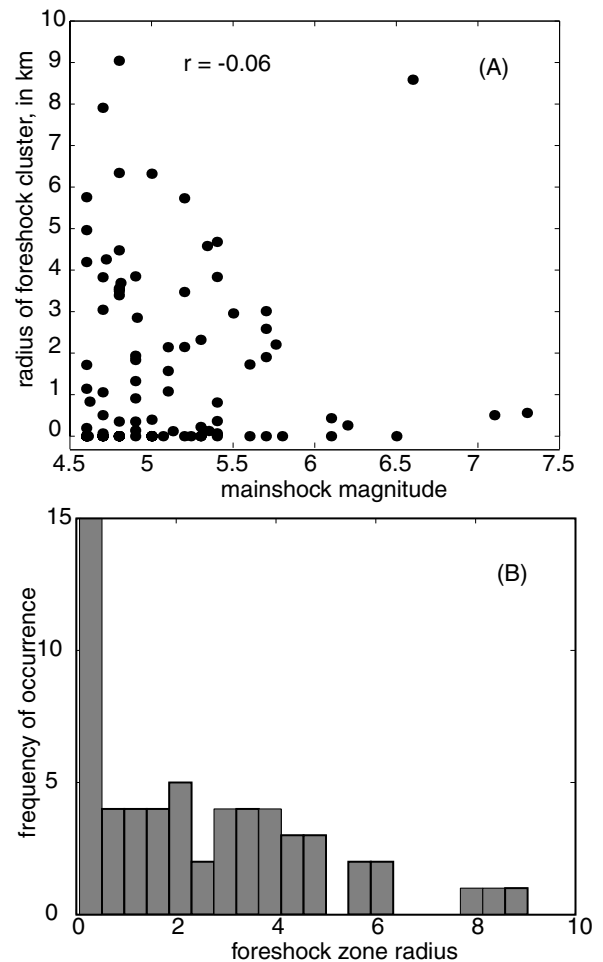


Figure 9. Mainshock magnitude is plotted versus the radius of the smallest circle capable of enclosing all of the foreshocks. No significant correlation is seen between mainshock magnitude and the area spanned by its foreshock sequence ($r = -0.06$ for 88 data points, a value that has a 58% probability of occurring by chance). (B) Histogram of the radii of the foreshock sequences plotted in (A) (omitting foreshock sequences containing only one event).

nitude M_1 varies as $c10^{\alpha M_1}$, where $\alpha = b = 1$, regardless of whether the magnitudes of the aftershocks are larger or smaller than M_1 . In addition, the number of aftershocks of magnitude $M_2 \pm \Delta M$ produced by a mainshock of magnitude M_1 is consistent with the hypothesis that the magnitude of each aftershock is chosen randomly from the Gutenberg–Richter distribution. These findings all support the idea that aftershocks, multiplets, and foreshocks are caused by the same physical process.

We have also tested whether the single-mode triggering model can be readily disproven. We have demonstrated that the doublet rate in the Solomon Islands, previously thought to be so high that it warranted a special physical mechanism, is in fact within the range predicted by the single-mode triggering model given the high aftershock rate in the region. It has also been claimed that foreshocks are not simply small mainshocks, but rather are triggered by the nucleation phase of the upcoming larger mainshock. If this is true, we would expect mainshock size to influence the magnitude, number, and/or spatial extent of the foreshocks. We do not observe any such correlations.

We conclude that statistical evidence strongly supports the idea that foreshocks, doublets, and aftershocks are simply different names for the same earthquake-triggering phenomena played out on different relative magnitude scales. This suggests that large-earthquake forecasting by identifying foreshock sequences in progress is not likely to become possible.

Acknowledgments

We would like to acknowledge helpful conversations with Tom Hanks, Agnes Helmstetter, and Greg Beroza. We are also thankful for comments from Priscilla Song, Meredith Nettles, Miaki Ishii, Mike Antolik, Jianfeng Pan, John Lin, James Wang, Colleen Dalton, Diana Valencia, and James Rice. Earthquake catalog data were made available by the Council of the National Seismic System, the Southern California Earthquake Data Center, the California Institute of Technology, the Northern California Earthquake Data Center, the Berkeley Seismological Laboratory, and the Northern California Seismic Network. Support for this work was provided by the Southern California Earthquake Center. SCEC is funded by NSF Cooperative Agreement EAR-0106924 and USGS Cooperative Agreement 02HQAG0008. The SCEC Contribution Number for this article is 719.

References

- Abercrombie, R. E., and J. Mori (1996). Occurrence patterns of foreshocks to large earthquakes in the western United States, *Nature* **381**, 303–307.
- Agnew, D. C., and L. M. Jones (1991). Prediction probabilities from foreshocks, *J. Geophys. Res.* **96**, 11,959–11,971.
- Båth, M. (1965). Lateral inhomogeneities in the upper mantle, *Tectonophysics* **2**, 483–514.
- Centroid Moment Tensor (CMT) Catalog, www.seismology.harvard.edu/CMTsearch.html (last accessed March 2003).
- Console, R., and M. Murru (2001). A simple and testable model for earthquake clustering, *J. Geophys. Res.* **106**, 8699–8711.
- Console, R., M. Murru, and A. Lombardi (2003). Refining earthquake cluster models *J. Geophys. Res.* **108**, 2468, doi 10.1029/2002JB002130.
- Dodge, D. A., G. C. Beroza, and W. L. Ellsworth (1995). Foreshock sequence of the 1992 Landers, California earthquake and its implications for earthquake nucleation, *J. Geophys. Res.* **100**, 9865–9880.
- Dodge, D. A., G. C. Beroza, and W. L. Ellsworth (1996). Detailed observations of California foreshock sequences: implications for the earthquake nucleation process, *J. Geophys. Res.* **101**, 22,371–22,392.
- Ellsworth, W. L., and G. C. Beroza (1995). Seismic evidence for an earthquake nucleation phase, *Science* **268**, 851–855.
- Felzer, K. R., T. W. Becker, R. E. Abercrombie, G. Ekstrom, and J. R. Rice (2002). Triggering of the 1999 M_w 7.1 Hector Mine earthquake by aftershocks of the 1992 M_w 7.3 Landers earthquake, *J. Geophys. Res.* **107**, 2190, doi 10.1029/2001JB000911.
- Gutenberg, B., and C. F. Richter (1944). Frequency of earthquakes in California, *Bull. Seism. Soc. Am.* **4**, 185–188.
- Hardebeck, J. L., J. J. Nazareth, and E. Hauksson (1998). The static stress change triggering model: constraints from two southern California aftershock sequences, *J. Geophys. Res.* **103**, 24,427–24,437.
- Helmstetter, A. (2003). Earthquake triggering driven by small earthquakes? *Phys. Rev. Lett.* **91**, 058501.
- Helmstetter, A., and D. Sornette (2002). Sub-critical and super-critical regimes in epidemic models of earthquake aftershocks, *J. Geophys. Res.* **107** 2237, doi 10.1029/2001JB001580.
- Helmstetter, A., and D. Sornette (2003). Foreshocks explained by cascades of triggered seismicity, *J. Geophys. Res.* **108**, 2457, doi 10.1029/2003JB002409.
- Hurukawa, N. (1998). The 1995 Off-Etorofu earthquake: joint relocation of foreshocks, the mainshock, and aftershocks and implications for the earthquake nucleation process, *Bull. Seism. Soc. Am.* **88**, 1112–1126.
- Ishimoto, M., and K. Iida (1939). Observations of earthquakes registered with the microseismograph constructed recently, *Bull. Earthquake Res. Inst. Tokyo Univ.* **17**, 443–478.
- Kagan, Y. Y., and L. Knopoff (1981). Stochastic synthesis of earthquake catalogs, *J. Geophys. Res.* **86**, 2853–2862.
- Kanamori, H., and D. L. Anderson (1975). Theoretical basis of some empirical relations in seismology, *Bull. Seis. Soc. Am.* **65**, 1073–1095.
- Kilb, D., J. Gombert, and P. Bodin (2000). Triggering of earthquake aftershocks by dynamic stress, *Nature* **408**, 570–574.
- Lay, T., and H. Kanamori (1980). Earthquake doublets in the Solomon Islands, *Phys. Earth. Planet. Interiors* **21**, 283–304.
- Michael, A. J., and L. M. Jones (1998). Seismicity alert probabilities at Parkfield, California, revisited, *Bull. Seism. Soc. Am.* **88**, 117–130.
- Mori, J. (1996). Rupture directivity and slip distribution of the M 4.3 foreshock to the 1992 Joshua Tree earthquake, southern California, *Bull. Seism. Soc. Am.* **86**, 805–810.
- Ogata, Y. (1988). Statistical models for earthquake occurrence and residual analysis for point processes, *J. Am. Stat. Assoc.* **83**, 9–27.
- Ohnaka, M. (1993). Critical size of the nucleation zone of earthquake rupture inferred from immediate foreshock activity, *J. Phys. Earth* **41**, 45–56.
- Reasenber, P. A. (1999). Foreshock occurrence before large earthquakes, *J. Geophys. Res.* **104**, 4755–4768.
- Reasenber, P. A., and L. M. Jones (1989). Earthquake hazard after a mainshock in California, *Science* **243**, 1173–1176.
- Schwartz, D. P., and K. J. Coppersmith (1984). Fault behavior and characteristic earthquakes: examples from the Wasatch and San Andreas fault zones, *J. Geophys. Res.* **89**, 5681–5698.
- Shaw, B. E. (1993). Generalized Omori law for aftershocks and foreshocks from a simple dynamics, *Geophys. Res. Lett.* **20**, 907–920.
- Tsapanos, T. M. (1990). Spatial distribution of the difference between the magnitudes of the mainshock and the largest aftershock in the circum-Pacific belt, *Bull. Seism. Soc. Am.* **80**, 1180–1189.
- Utsu, T. (1961). A statistical study on the occurrence of aftershocks, *Geophys. Mag.* **30**, 521–605.
- Vere-Jones, D. (1966). A Markov model for aftershock occurrence, *Pure App. Geophys.* **64**, 31–42.

- Woo, G. (1996). Kernel estimation methods for seismic hazard source modeling, *Bull. Seism. Soc. Am.* **86**, 353–362.
- Xu, Z., and S. Y. Schwartz (1993). Large earthquake doublets and fault plane heterogeneity in the northern Solomon Islands subduction zone, *Pure Appl. Geophys.* **140**, 365–390.
- Yamanaka, Y., and K. Shimazaki (1990). Scaling relationship between the number of aftershocks and the size of the mainshock, *J. Phys. Earth* **38**, 305–324.

Department of Earth and Planetary Sciences
Harvard University
20 Oxford St.
Cambridge, Massachusetts 02138
(K.R.F., G.E.)

Department of Earth Sciences
Boston University
685 Commonwealth Ave.
Boston, Massachusetts 02215
(R.E.A.)

Manuscript received 10 April 2003.